ELSEVIER

Journal of Hydrology 235 (2000) 12–26

Journal of Hydrology

www.elsevier.com/locate/jhydrol

# Estimation of hydraulic parameters of shaly sandstone aquifers from geoelectrical measurements

O.A.L. de Lima[a,*], Sri Niwas[b]

[a]*Center for Research in Geophysics and Geology (CPGG)-Federal University of Bahia, Campus Universitário da Federação, Salvador, Bahia 40170-290, Brazil*

[b]*Department of Earth Sciences, University of Roorkee, Roorkee 247 667, India*

Received 5 October 1999; revised 7 March 2000; accepted 6 April 2000

**Abstract**

Electrical and hydraulic conductivities of shaly sandstones are described using a capillary approach for a granular, clay bearing material. The clays are assumed to occur as shale shells uniformly coating the insulated sand grains. The real and imaginary components of the complex electrical conductivity for this material model are written in terms of a unique solid matrix conductivity, treated as a volumetric property. Above a critical salt concentration the conductive contribution of the shells is independent of the electrolyte salinity. Under this condition the equation for the bulk conductivity of the sandstone can be expressed in a simplified form. However, *below* the critical concentration the matrix conductivity is dependent on the conductivity of the water saturating the shaly component and can be expressed only by the complete equation. The hydraulic conductivity for this model is expressed by a modified Kozeny–Carman equation. A new semi-empirical equation relates the hydraulic conductivity for such rocks, to their porosity, formation resistivity factor and the electrical conductivity of its solid matrix. These combined properties are described as the lithoporosity factor. In this new formulation the petrophysical parameters involved are easily determined from the electrical geophysical measurements. The performance of this equation is firmly tested with experimental laboratory data available in the literature. Its application is then extended to estimate the hydraulic parameters of a shaly sandstone aquifer in Bahia-Brazil, using either the borehole *or* the surface geoelectrical data. Examples are given to emphasize the combined use of electrical resistivity and induced polarization measurements in computing hydraulic properties. 

*Keywords*: Permeability; Electrical conductivity; Induced polarization; Shaly sand-stones; Geophysical logging

## 1. Introduction

The knowledge of the spatial distribution of hydraulic parameters of a groundwater flow domain is essential both for optimizing aquifer exploration programs as well as to evaluate the *efficiency* of contaminant *remediation* processes. To model the aquifer behavior one needs to solve a set of differential equations under appropriate boundary conditions. In the absence of exact solution of these equations, numerical solutions are sought by subdividing the aquifer in many blocks of elementary dimensions. For heterogeneous aquifers the procedure of assigning the hydraulic parameters of each element is not obvious.

Analysis of pump test data as a function of time are classical procedures for estimating aquifer parameters. These results suffer from non-uniqueness

* Corresponding author.

*E-mail addresses:* olivar@cpgg.ufba.br (O.A.L. de Lima), srsnpfes@rurkiu.ernet.in (Sri Niwas).

0022-1694/00/$ - see front matter 
PII: S0022-1694(00)00256-0

and because of physical and conceptual constraints underlying such tests, the interpreted results represent macroscopic averages taken over large volumes of the porous medium. Small-scale textural and structural variabilities are lost in this process and these details may be necessary to solve the hydrological problem efficiently.

Geophysical measurements made within wells or at Earth's surface sample small formation volumes, typically within a decimetric to a decametric scale. The physical conditions (tortuosity and porosity) controlling the electric current flow (electrical *resistivity*) also likewise *control* the lateral flow of the water (hydraulic conductivity) in porous *media*. Exploiting this similarity, a large number of empirical equations has been developed to convert the geophysical measurements into hydraulic parameters (Kelly, 1977; Kosinski and Kelly, 1981; Scott, 1988; Sen et al., 1990; Börner et al., 1996; Sighal et al., 1998; Yadav and Abolfazli, 1998). Sri Niwas and Singhal (1981, 1985) have developed an analytical relationship between the hydraulic conductivity and electrical resistivity through the well-established laws of physics, i.e. Darcy's law of lateral flow of ground water and Ohm's law of current flow in clean porous media. *These* results *provide* a physical and mathematical basis to the statistically established relations.

For clean sandstones, a porous model of free rugose channels leads to a fractal representation for its porosity, specific surface, hydraulic and electrical tortuosities as well as to its formation resistivity factor (Katz and Thompson, 1985; Korvin, 1992; Turcotte, 1992). In this model the grain size distribution is such that most of the void space is hydraulically interconnected and almost the whole interstitial fluid is free to flow under an applied piezometric head. This interconnected porosity may be *referred* to as an effective hydraulic porosity ($\phi_e$). The mean geometrical tortuosity of the channels can be distinguished as a free pore tortuosity having similar effects on both the electrical and hydraulic flows through the medium. For such rocks analytical and experimental *evidence* support a relationship between the electrical and hydraulic conductivities obtained from Archie's and Kozeny–Carman's equations in the following form (Croft, 1971; Kelly, 1977)

$$k = \alpha F^{-q}, \tag{1}$$

where $\alpha$ and $q$ are empirical constants and $F$, the formation resistivity factor, is given as $F = \sigma_w/\sigma_0$, with $\sigma_0$ and $\sigma_w$ being the conductivities of the fully saturated whole rock and of its pore electrolyte, respectively. The constant $\alpha$ in Eq. (1) is inversely proportional to the square of the specific surface for the sandstone, and so has a dimension of $L^2$.

It is worthwhile to recall here that Heigold et al. (1980) have combined Darcy's equation and Archie's relation (Archie (1950)) between permeability and porosity of rocks to obtain the following equation similar to Eq. (1) as

$$k = a_1 \phi^{b_1}, \tag{2}$$

where $k$ is the intrinsic permeability ($m^2$)—the pore area of the rock governing the flow, $\phi$ is porosity and $a_1$ and $b_1$ are constants. However, the hydrophysical property is the hydraulic conductivity, $K$ (m/s)—fluid velocity, which depends on both *the* formation and *the* fluid contained in it. Notwithstanding, our effort should be to obtain a more physically supported quantitative relation instead of an empirical one.

Nuttings' equation (Hubbert, 1940) relates $k$ and $K$ as

$$K = k\frac{\rho g}{\mu}, \tag{3}$$

where $\mu$ is the dynamic viscosity of the fluid (kg/ms), $\rho$ the fluid density ($kg/m^3$) and $g$ the acceleration due to gravity ($m/s^2$). For hydrological problems the fluid is water and *ideally* $\mu$ and $\rho$ can be taken as unit. Thus the permeability value can be converted *approximately* to hydraulic conductivity *by* multiplying by 10.

In shaly sandstones, however, there are two main grainsize populations, one characterizing the sand fraction and another the shaly portion. This generates two porosity parameters: one effective hydraulic porosity, as for the clean sandstone, and a shale porosity whose pores are normally filled with bound water. In the same way, we can distinguish two tortuosity indices: one for the free water channels and another for the bound water conduits. The first controls a large fraction of the electrical flow and the whole of the hydraulic transport through the medium. However, the second one, contributes only to the electrical transport inside the shaly coatings. These two electrical paths act essentially in a parallel association (de Lima and Sharma, 1990). Pure shales represent the

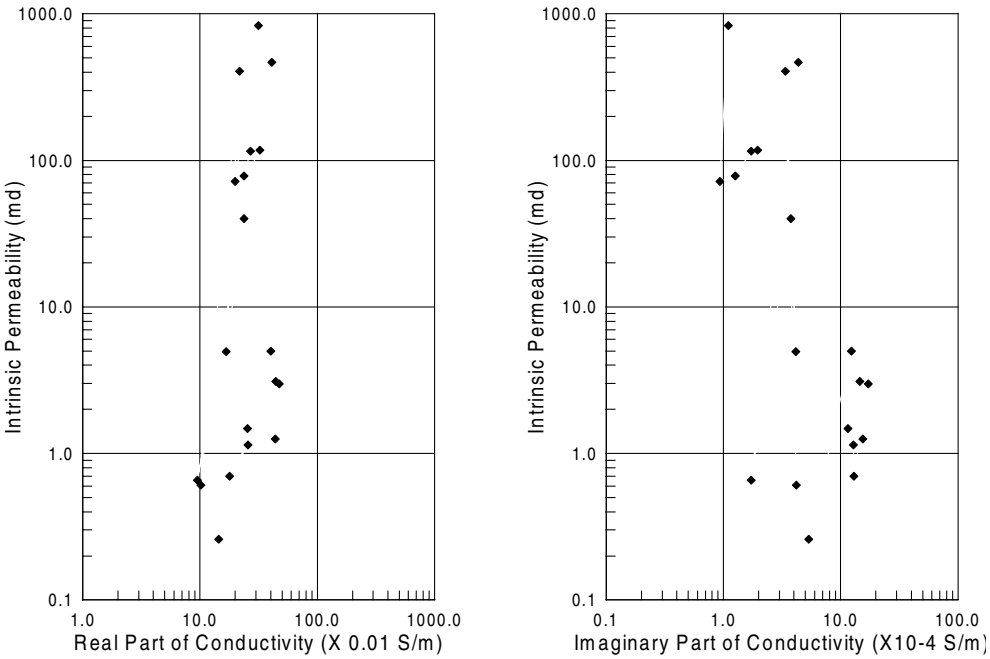


Fig. 1. Relationship between intrinsic permeability and real and imaginary component of the electrical conductivities at 0.5 M NaCl electrolyte salinity for typical shaly sandstones (data from Vinegar and Waxman (1984), 1984).

limits when $\phi_e \rightarrow 0$, when one still has effective electrical conduction but the medium may be almost impervious to water flows.

For shaly sandstone there is no straightforward relationship between electrical and hydraulic conductivities. In Fig. 1 we plot the intrinsic permeability data of Vinegar and Waxman (1984) for typical shaly sandstones, against their corresponding real and imaginary electrical conductivity components. From this figure we observe no obvious correlation between electrical and hydraulic parameters.

de Lima (1995), using a capillary approach for a granular shaly coated model, has derived a semi-empirical equation relating the intrinsic permeability of a porous medium to its porosity, formation factor and clay content as follows:

$$k = \alpha_0 \left[ \frac{\phi_e F^{-1}}{1 + \delta Q_v} \right]^q, \tag{4}$$

where $\alpha_0$ and $q$ are also empirical constants, $\phi_e$ and $F$ are the effective porosity and true formation factor of the sandstone, $\delta (= \bar{r}_s / 3\bar{a}\beta_1)$ is a parameter controlled by the average sizes of the sand and clay particles $(\bar{r}_s, \bar{a})$ and the particular type of clay ($\beta_1$ is the charge density on a clay particle) and $Q_v$ is the clay compensating ionic charge per unit pore volume of the sandstone (de Lima, 1995).

Existing hydrophysical models have not used the surface conduction effects and differences in tortuosities to estimate the total surface area contributed by shale/clay in an aquifer. At the same time results using relations developed for clean formations remain questionable for use in shaly formations. This situation requires that we widen the canvas by including other geoelectrical data in addition to resistivity measurements to redeem this hopeless situation.

In the present work we review the petrophysical basis for relating electrical and hydraulic parameters of a granular material having dispersed charged particles in its solid matrix. By reworking and expanding previous results for self-similar clay-coated models described by de Lima and Sharma (1990, 1992) and de Lima (1995) we developed a new permeability equation totally dependent on petrophysical parameters easily determined either from the surface electrical or well log measurements. For borehole logging the electrical resistivities measured with different

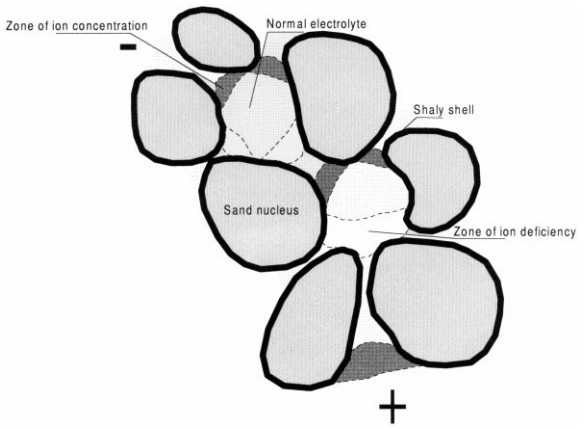


Fig. 2. Sketch of a self-similar granular shaly sandstone model and one of its representative channel.

depths of investigation are required to find the necessary parameters. From surface electrical measurements the dc-resistivity and an induced polarization parameter are used for the conversion. Although the IP phenomenon has been suggested to correlate with the aquifer permeability (Bodmer et al., 1968; Ogilvy and Kuzmina, 1972; Worthington and Collar, 1984; Börner et al., 1996; Weller and Börner, 1996), to our knowledge, this is the first report describing a firmly supported quantitative use of IP and resistivity for an aquifer evaluation.

## 2. The shaly sand model

The electrical, hydraulic and other transport properties of shaly sandstones are strongly controlled by the geometrical arrangement of their grains, by the interfacial processes occurring at boundaries between water and clay particles, as well as by the saturation level and the salinity of the interstitial water.

To simulate the physical behavior of shaly sandstones we assume a self-similar porous model of spheroidal particles composed of $n_s$ insulating sand grains of distributed sizes $r_{s,i}$, and $n_i$ clay particles also of distributed sizes $a_i$ and arranged essentially as thin uniform coating structures around the sand grains. The clays are electrically charged particles that are compensated by exchangeable cations. Under a water wet condition these ions form diffuse atmospheres around the clays. Fig. 2 is a schematic representation of this granular model outlining one typical porous channel. Such a channel is characterized by wide pore bodies sequentially interconnected through narrow pore throats.

The coating shaly structure also alters the effective porosity and the electrical and hydraulic tortuosities within the representative channel. An increase in the clay proportion tends to reduce the effective free pore diameter and to increase the electrical tortuosity of the bound water conduits around the pore walls. These will also introduce important effects on the hydraulic conductivity of this porous medium. In the following sections we will describe the basic electrical and hydraulic characteristics of this granular shaly coated sandstone.

### 2.1. The electric effects

The electrical conductivity changes introduced by clays have been described by several authors (Vacquier et al., 1957; Marshall and Madden, 1959; Vinegar and Waxman, 1984; de Lima and Sharma, 1990). The main enhancement is caused by the local ionic concentration gradients developed by membrane filtration effects along constrictions on their pore channels.

Two characteristic lengths are distinguished in the assumed granular model (Fig. 2): a free pore length at the grain-size scale and a pore throat constriction of smaller dimension. An external electrical field will induce differentiated ionic fluxes inside this channel that, along the constrictions, are opposed by the cationic selectivity of the clays. These filtration effects will change the local ionic distribution along the pore channel. An ionic depletion is induced at the positive side of a constriction whereas a corresponding concentration is developed on its negative side. These charge accumulations make the electrical conductivity of such sandstones frequency dependent, described by a total complex current conductivity function (Dias, 1972; Klein and Sill, 1982; de Lima and Sharma, 1992). These are the main cause of the induced polarization effects observed in shaly sandstones (Vacquier et al., 1957; Marshall and Madden, 1959).

Next, we will assume that for low frequency ranges (such that $\sigma^* \gg \omega\epsilon^*$) the complex electrical conductivity of a shaly sandstone is given by a

Bruggeman–Hanay type equation in the form

$$\sigma_0^* = \sigma_w \phi_e^m \left( \frac{1 - \sigma_{cs}^*/\sigma_w}{1 - \sigma_{cs}^*/\sigma_0^*} \right)^m, \quad (5)$$

where $\phi_e$ is the effective medium porosity and $m$ a non-dimensional parameter that depends on the average aspect ratio of the coated sand grains; $\sigma_0^*$ and $\sigma_{cs}^*$ are the complex conductivities of the sandstone and of the clay-coated sand grains, and $\sigma_w$ the real conductivity of the electrolyte (de Lima and Sharma, 1992).

For low frequency ranges and for a dominant electrical conduction through the porous electrolyte ($\sigma_w \gg |\sigma_{cs}|$) a binomial expansion on both the numerator and denominator of Eq. (5) and retention of only first order terms gives

$$\sigma_0^* = \frac{1}{F}[\sigma_w + m(F-1)\sigma_{cs}^*], \quad (6)$$

where $F$ is the usual Archie's formation factor ($F = \phi_e^{-m}$). Eqs. (5) and (6), with appropriate substitutions, can also be applied to compacted clays and pure shales. In this case, $\sigma_0^*$ will represent $\sigma_{sh}^*$ and $\sigma_{cs}^*$ will be replaced by the complex conductivity of wetted clay particles $\sigma_c^*$.

The clay or the coated-clay conductivity will, in general, be dependent on the conductivity of its interstitial electrolyte. However, as the effective porosity of clay aggregates and shales is very small, the conductivity of their bond waters soon assume a constant value independent of the water salinity of the free pore electrolyte (Clavier et al., 1997). Eq. (6) includes the following components:

$$\sigma_{0,R} = \frac{1}{F}[\sigma_w + m(F-1)\sigma_{cs,R}], \quad (7)$$

and

$$\sigma_{0,I} = m(1 - 1/F)\sigma_{cs,I}, \quad (8)$$

where the subscripts R and I stands for real and imaginary components of the complex conductivity function.

For a clay-coated spherical particle representative of a shaly sandstone, and under the same low frequency range, we have from de Lima and Sharma (1992)

$$\sigma_{cs}^* = \frac{2p}{3-p}\sigma_{sh}^*, \quad (9)$$

where $\sigma_{sh}^*$ is the complex conductivity of a shaly shell and $p$ is the clay volume fraction in the sandstone matrix. For spheroidal shaly coated particles we may use Fricke's result (Fricke, 1924) given as

$$\sigma_{cs} = \frac{wp}{w + 1 - p}\sigma_{sh}, \quad (10)$$

where $w$ is a shape factor. For small values of $p$ ($p < 0.3$) Eqs. (9) or (10) allows to write

$$\sigma_{cs,R} = \gamma p \sigma_{sh,R}, \quad (11)$$

where $\gamma$ is also a geometrical constant ranging from 0.5 to 1. In cases where clays occurs as discrete particles dispersed through the sandstone matrix, de Lima and Sharma (1990) also found that $\sigma_{cs} = p\sigma_{sh}$. Thus, we have good support for using Eq. (11) to express $p$ in terms of the ratio between the effective grain conductivity and the conductivity of its shaly coating.

Further, for low porosity clays or shales and at low frequency measurements, the following approximations hold (de Lima and Sharma, 1992)

$$\sigma_{sh,R} = \frac{\delta_1(1 + \delta_1 A)}{(1 + \delta_1 A)^2 + \delta_1^2 B^2}\sigma_w, \quad (12)$$

and

$$\sigma_{sh,I} = \frac{\delta_1^2 B}{(1 + \delta_1 A)^2 + \delta_1^2 B^2}\frac{\sigma_w}{\omega}, \quad (13)$$

where $\delta_1 = \beta_1/aC_1$, $\beta_1$ being the surface counterion density around a clay particle of radius $a$, and $C_1$ is the cationic concentration in the electrolyte where the coated spheres are immersed; $A$ and $B$ are parameters dependent on frequency and the relaxation time of the charged clays. From Eqs. (12) and (13) we can write

$$\sigma_{sh,I} = \frac{\delta_1 B}{\omega(1 + \delta_1 A)}\sigma_{sh,R}. \quad (14)$$

Combining Eqs. (14) and (9) we get

$$\sigma_{cs,I} = \frac{\delta_1 B}{\omega(1 + \delta_1 A)}\sigma_{cs,R}. \quad (15)$$

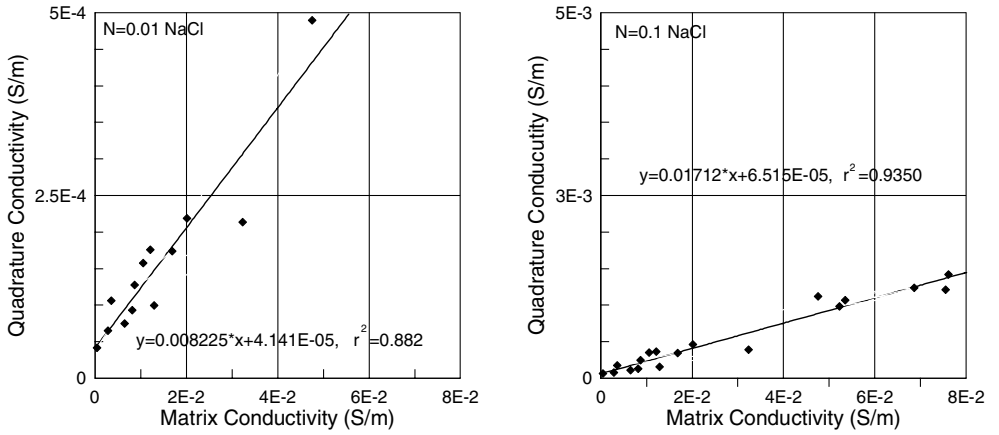


Fig. 3. Imaginary component of the bulk conductivity of shaly sandstones versus the real component of its matrix conductivity for 0.01 and 0.1 M NaCl electrolytes (data from Vinegar and Waxman (1984), 1984).

Finally, substituting Eq. (15) in Eq. (8) we have

$$\sigma_{0,\mathrm{I}} = \frac{m(1 - 1/F)\delta_1 B}{\omega(1 + \delta_1 A)}\sigma_{\mathrm{cs,R}} = \lambda_q \sigma_{\mathrm{cs,R}}, \qquad (16)$$

where $\lambda_q$ is a non-dimensional parameter dependent on the geometrical features of the porous medium, on the clay species present in the shaly shells and on the frequency.

Eq. (16) shows that the imaginary component of the complex conductivity of a shaly sandstone depends linearly on the real component of the volumetric conductivity of its solid matrix. The constant of proportionality is a geometrical parameter slightly dependent on the frequency and on the clay type in the sandstone matrix.

Thus, by treating the electrical conductivity of a shaly sandstone as a complex parameter we derive explicit expressions relating the real and imaginary components of its bulk conductivity to the real component of the conductivity of its solid matrix. Now, we have two alternative procedures to find ($\sigma_{\mathrm{cs,R}}$) from geoelectrical measurements: using Eq. (7) and the real component of conductivity measurements; and using Eq. (16) and the imaginary component of conductivity measurements or an induced polarization parameter, as we will show below.

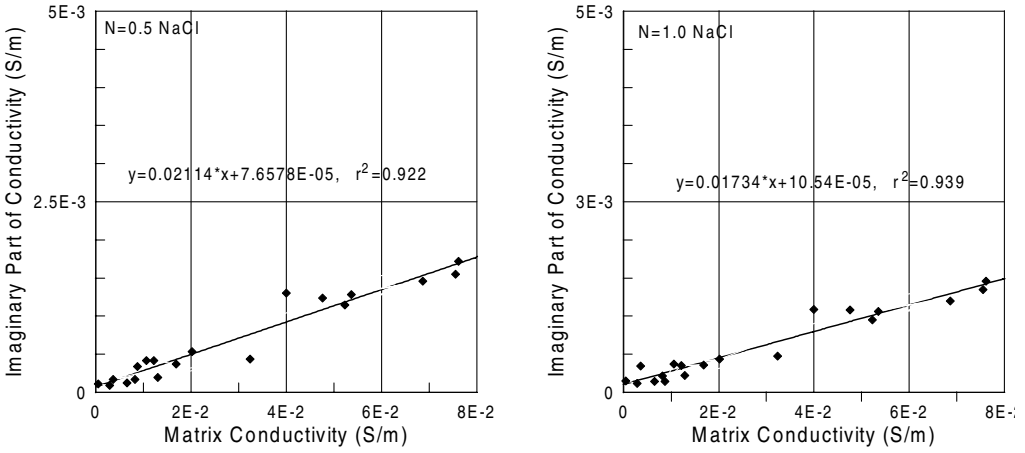


Fig. 4. Imaginary component of the bulk conductivity of shaly sandstones versus the real component of its matrix conductivity for 0.5 and 1 M NaCl electrolytes (data from Vinegar and Waxman (1984), 1984).

In Figs. 3 and 4 we present the best correlation results between the imaginary component of the conductivity of shaly sandstones measured by Vinegar and Waxman (1984) as a function of their grain volume conductivity. These were determined from straight-line fits to their bulk real component measurements made with different water salinities. The figures show high levels of correlation ($r^2$ between 0.89 and 0.94) and that $\lambda_q$ varies slightly from 0.00822 at 0.01 N to 0.01734 at 1 N. The fittings show very small intercepts of about $4.1–10.5 \times 10^{-5}$ S/m, attesting the general validity of Eq. (16).

The detection of IP effects in the time domain is made by measuring both the maximum voltage during the charging period of a dc-current flow, and the transient decay of the electrical potential as a function of time, after the current is turned off. The maximum voltage is used to compute an apparent resistivity function ($\rho_a$). The normalized integration of the decaying voltage at a specified time window gives an apparent, time-dependent, chargeability ($M_a$) for that window as

$$M_a(t) = \frac{1}{V_0 \Delta t} \int_{t_1}^{t_2} V_{IP}\, dt. \tag{17}$$

where $\Delta t = t_2 - t_1$ is the width of the window and $V_0$ is the maximum voltage observed during the charging period. With modern instrumentation, the usual practice is to sample the decaying voltage through a sequence of windows. In each window a partial apparent chargeability is measured. These values are then used to compute an weighted average chargeability for the decaying period.

In the frequency domain both the amplitude and the phase shift of the apparent impedance of the earth is measured using different frequencies. A frequency effect (FE) can be evaluated by comparing the amplitude measurements made at a high alternating frequency with the one from a much lower frequency taken as a dc value

$$FE = \frac{|\rho^*(\omega_1)| - |\rho^*(\omega_2)|}{|\rho^*(\omega_2)|}, \tag{18}$$

with $\omega_1 \ll \omega_2$. An alternative procedure uses the phase shift measurement made at an intermediate frequency as (Shuey and Johnson, 1973; Vinegar and Waxman, 1984)

$$FE(\omega_1, A\omega_1) = -\frac{2}{\pi}\theta(\omega_1\sqrt{A}) \ln A, \tag{19}$$

with $A$ being the ratio between the two used frequencies and $\theta = \tan^{-1} \sigma_{0,I}/\sigma_{0,R}$ is measured in milliradians.

As the IP phenomenon is a linear one the time domain and the frequency domain data are theoretically related by Fourier transforms. To a first approximation we may use in practice the following result relating the peak chargeability $M(0)$ to the maximum FE effect (Zonge et al., 1972)

$$FE = \frac{M(0)}{1 - M(0)}. \tag{20}$$

### 2.2. The hydraulic effect

The intrinsic permeability of a porous medium (dimension $L^2$) is a measure of its frictional resistance to a single-phase fluid flowing through it. It depends on the pore size distribution, on the roughness and constrictions of pore space and on the tortuosity and connectivity of their internal pore channels. The most extensively used approach to simulate the hydraulic behavior of granular rocks is through the Kozeny–Carman theory. In this approach, the granular porous medium is statistically modeled as a spatial array of capillary channels having different lengths and cross-sections. Theoretical and experimental results have attested the practical validity of such approximation (Wyllie and Spangler, 1952; Terzaghi, 1955; Haring and Greenkorn, 1970; Scheidegger, 1974; Brace, 1977; Wong et al., 1984; Clennell, 1997).

Following de Lima (1995) we start from the Kozeny–Carman equation, derived for a porous medium modeled as a bundle of sinuous capillary channels, given as

$$k = \alpha \phi_e \left( \frac{V_P}{S_A \tau_h} \right)^q, \tag{21}$$

where $\alpha$ is a dimensionless shape factor related to the statistical average of the channel perimeter to its cross-sectional area, $\phi_e$ is the effective porosity, $S_A/V_P$ is the specific surface area referred to the effective pore volume, and $\tau_h$ is an average hydraulic tortuosity for the medium. The constant $\alpha$ for nearly uniform

pore size distributions is about 0.5 (Carman, 1956). The fractional exponent $q$ in Eq. (21) is required to take into account the fractal nature of the pore space of a real porous rock.

From Fig. 2 we assume, as was performed by de Lima (1995), that the hydraulic tortuosity of such a model can be approximated by the mean electric tortuosity of the free pore channels, given as

$$\tau = \phi_e^{(1-m)}. \tag{22}$$

The conductive contribution due to the shaly shells is described by a different tortuosity referred as the bound-water tortuosity $\tau_b = (1-\phi_e)/m(1-\phi_e^m)$ (de Lima and Sharma, 1992). Eq. (22) has been derived for clean sandstones, by combining the definitions of Archie's formation factor and Carman's hydraulic tortuosity (Wyllie and Rose, 1950; Winsauer et al., 1952). The similarity between hydraulic and electric tortuosities has been also pointed out by Clennell (1997) and many others. A similar approach has been implicitly used by Mualem and Friedman (1991) and Weerts et al. (1999) for modeling the bulk soil electrical conductivity of saturated and unsaturated soils.

The specific surface for the model may be computed as follows. A representative sample of volume $\Delta V_0$ of the model contains $n_s$ sand grains and $n_c$ clay particles. Two classes of pore space exist: one, of dimension in the sand-size scale, contributes to the effective porosity, $\phi_e$; another, within a clay-size dimension, characterizes the shale porosity, $\phi_{sh}$. If $p$ is the shale volume fraction, the total porosity, $\phi$, for this sample is

$$\phi = \phi_e + p\phi_{sh}(1-\phi_e). \tag{23}$$

The effective void volume in the sample is

$$\Delta V_v^{cs} = \frac{\phi_e}{1-\phi_e}\Delta V_{cs}, \tag{24}$$

where $\Delta V_{cs}$ is the volume fraction occupied by the shaly coated matrix. For spherical particles

$$\Delta V_{cs} = \frac{4}{3}\pi\frac{\phi_e}{1-\phi_e}\sum_{i=1}^{n_s} r_{cs,i}^3. \tag{25}$$

The total solid surface area exposed to fluid in this granular model is

$$\Delta A_{s,c} = 4\pi\left[\sum_{i=1}^{n_s} r_{s,i}^2 + \sum_{i=1}^{n_c} a_i^2\right]. \tag{26}$$

With $p$ given as

$$p = 1 - \Delta V_s/\Delta V_{cs},$$

and

$$\Delta V_c = p(1-\phi_{sh})\Delta V_{cs}$$

we may write the following relations:

$$\sum_{i=1}^{n_s} r_{cs,i}^3 = \frac{\sum_{i=1}^{n_s} r_{s,i}^3}{1-p} = \frac{\sum_{i=1}^{n_c} a_i^3}{p(1-\phi_{sh})}. \tag{27}$$

Using the above relations, the specific surface area related to the effective pore volume of the sample (dimension $L^{-1}$) can be written as

$$S_{s,c} = \frac{S_A}{V_P} = S_s\left[1 + p(1-\phi_{sh})\frac{\bar{r}_s}{\bar{a}}\right], \tag{28}$$

where $S_s = 3(1-\phi_e)/\phi_e\bar{r}_{cs}$ is the specific surface area of a clean sandstone of the same texture and porosity, and $\bar{r}_{cs}$, $\bar{r}_s$ and $\bar{a}$ are the harmonic averages for the coated sands, the sand cores and the clay sizes, respectively. Eq. (28) has been obtained on the assumption of small values of $p$ and $\phi_{sh}$ such that products containing the square of these quantities were neglected. For many shaly sandstones, there is a direct relation between their matrix electrical conductivity, the shale proportion and the shale conductivity, allowing to rewrite Eq. (28) as

$$S_{s,c} = S_s(1 + \delta_c\sigma_{cs,R}), \tag{29}$$

where $\delta_c = (1-\phi_{sh})\bar{r}_s/\bar{a}\gamma\sigma_{sh}$ depends on the properties of the clay components and the average size of the sand fraction.

For montmorillonite and kaolinite gels in distilled water, experimental data from Cremers and Laudelout (1966) allow us to find the minimum values for the electrical conductivity for these compacted wet clays as $\sigma_c^{mont} = 0.703$ S/m and $\sigma_c^{kao} = 0.083$ S/m (de Lima and Sharma, 1990). For a critical conductivity of the electrolyte saturating the shaly shells of 2.5 S/m, a shaly porosity in the range of 20–30%, and an averaged representative grain size ratio $\bar{r}_s/\bar{a} = 200$ we find $\delta_c$ varying from 30 to 150 m/S,

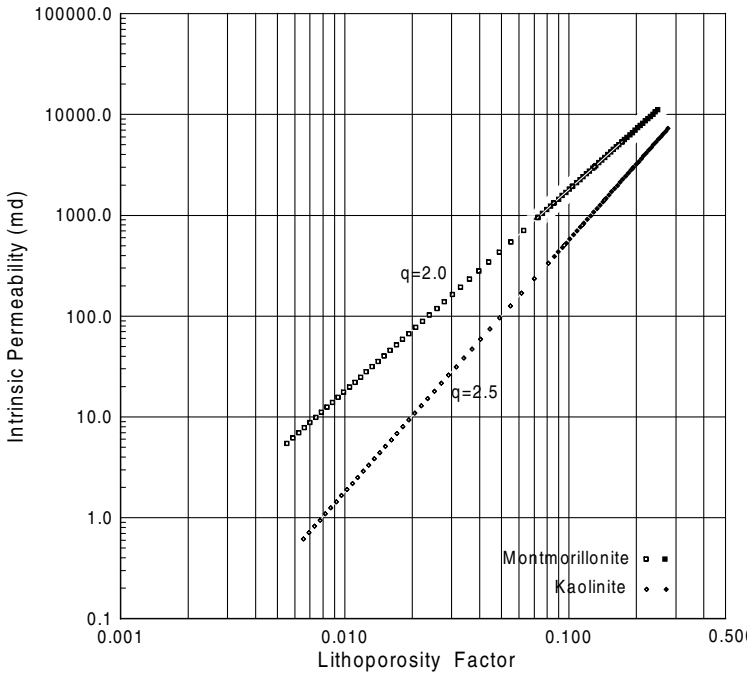


Fig. 5. Theoretical intrinsic permeability versus the lithoporosity factor for typical shaly sandstone models.

respectively, for montmorillonite and kaolinite aggregates or shales.

Combining the results expressed by Eqs. (22) and (29) into Eq. (21) we obtain

$$k = \alpha_0 \left[ \frac{\phi_e^{(m-1+1/q)}}{1 + \delta_c \sigma_{cs}} \right]^q, \tag{30}$$

where $\alpha_0 = \alpha/S_s^q$ has a topological dimension $L^2$, $\delta_c$ is a lithologic parameter dependent on the particle size distributions for sands and clays, and the exponent $q$ is expected to depend on the coated particle shapes and the packing structure of the sandstone. In general, $\alpha_0$ varies from about 180,000 $\mu m^2$ in fine grained ($\bar{r}_{cs} =$ 100 $\mu$m) to 50,000 $\mu m^2$ in medium grained ($\bar{r}_{cs} =$ 300 $\mu$m) shaly sandstones and $q$, the space filling fractal dimension, is in the range from 2 to 3.

To show the effect of changes on the characteristic parameters of Eq. (30) we constructed Fig. 5. Starting from a clean sandstone of initial effective porosity of 35% we add, in steps, small amounts of clays up to a maximum $p = 20\%$, ending with a shaly sandstone of $\phi_e = 18.75\%$. Two types of clays are specified by $\sigma_{sh}^{(1)} = 0.078$ S/m and $\sigma_{sh}^{(2)} = 0.685$ S/m. The grain size distributions are such that we have two distinct values of $\delta_c$ equal to 50 and 200 m/S. In Fig. 5 we plot in a log–log scale the modeled permeability values against a lithoporosity factor for shaly sandstones defined as $L_{\phi_e} = \phi_e^{(m-1+1/q)}/(1 + \delta_c \sigma_{cs})$. We can see from the figure that the effect of a change in $\delta_c$ is to displace the span of the permeability–lithoporosity relationship. The exponent $q$ determines the inclination of the straight line segments, whereas $\alpha_0$ defines the starting point at $\sigma_{cs} \rightarrow 0$ and $\phi_e \rightarrow 1$.

### 2.3. Experimental results

The permeability Eq. (30) has been tested with experimental core data published by Vinegar and Waxman (1984). This data set includes sandstone samples representative of different US oil fields. The measurements were made under controlled conditions, at five different NaCl electrolyte resistivities, covering a range from 0.07 to 8.5 $\Omega$ m. Thus, they include both saline and fresh water electrolytes. Values of $\sigma_{cs}$ and $F$ were determined from linear best fitting the real component of their electrical conductivity measurements. The effective porosity

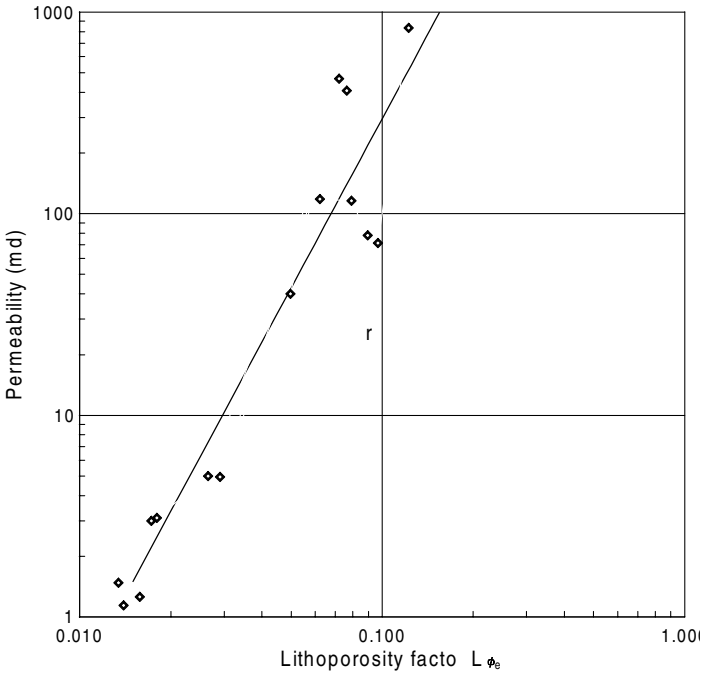


Fig. 6. Relationship between the intrinsic permeability and lithoporosity factor for shaly sandstone (data from Vinegar and Waxman (1984).

$\phi_e$ of each sample has been computed from the $F$ values using an average m for the data set that includes only the samples for which the intrinsic permeability is above 1 md. As the clays in the samples were described as mixtures of kaolinite, illite and montmorillonite we estimated $\delta_c$ to be between 50 and 100 m/S. Eq. (30) was fitted to their experimental data by plotting log(k) versus log($L_{\phi_e}$) as shown in Fig. 6 for $\delta_c = 100$ m/S. The best fit linear routine gives $\alpha_0 = 180,\ 015$ md and $q = 2.78$ with a regression coefficient $r^2 = 0.9054$. Two other values for $\delta_c$ were used with the same data. For $\delta_c = 50$ we find $\alpha_0 = 299,\ 610$ md, $q = 3.51$ and $r^2 = 0.9183$. For $\delta_c = 200$ m/S we obtain $\alpha_0 = 181,\ 920$ md, $q = 2.35$ and $r^2 = 0.8895$. From these results we find the data can be satisfactorily described by assuming $\delta_c = 100$.

Although the adjusted parameters are naturally not universal, they may be taken as characteristics for a wide class of shaly sandstones. If so, they can be used for initial estimates of the order of magnitude of the intrinsic permeability of shaly formations. In this way, the determined parameters were applied in this work as first approximations to estimate the intrinsic permeability of the São Sebastião aquifer using well log and surface electrical geophysical measurements.

The São Sebastião Formation is one of the most important aquifer in the Recôncavo Basin, Bahia—Brazil. It is composed of thick shaly sandstones having interlayered shales and siltstones. The sandstones were formed as stacked channel and bar deposits of a large braided alluvial environment. The shales and siltstones are lacustrine deposits related to rapid flooding episodes within a tectonically active intracontinental basin (de Lima, 1993). Fig. 7 shows the statistical distribution of porosities and permeabilities measured on 53 sandstones samples selected from drill cores of a deep well drilled to a depth of 1025 m. The measured porosities range from 18.8 to 34.9%, with a median of 25.7%. Their permeabilities cover a wide spectrum having a bimodal logarithmic distribution ranging from less than 100 to 2750 md, with a median of 794 md.

Fig. 8 shows the geophysical log of a water production well drilled in the São Sebastião Formation in Recôncavo Basin, Bahia, Brazil. The log suite consists of: (i) the deep induction and the short normal resistivity curves responding to both the virgin

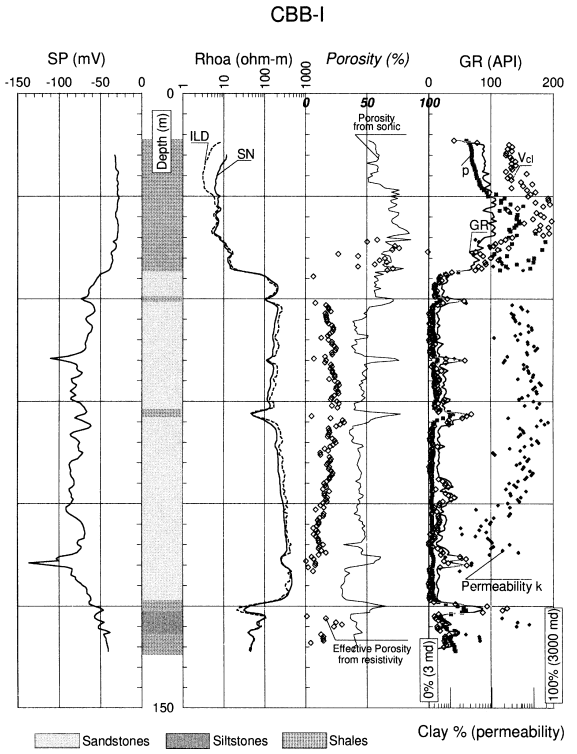


Fig. 7. Frequency distribution of porosity and permeability for shaly sandstones of the São Sebastião Formation.

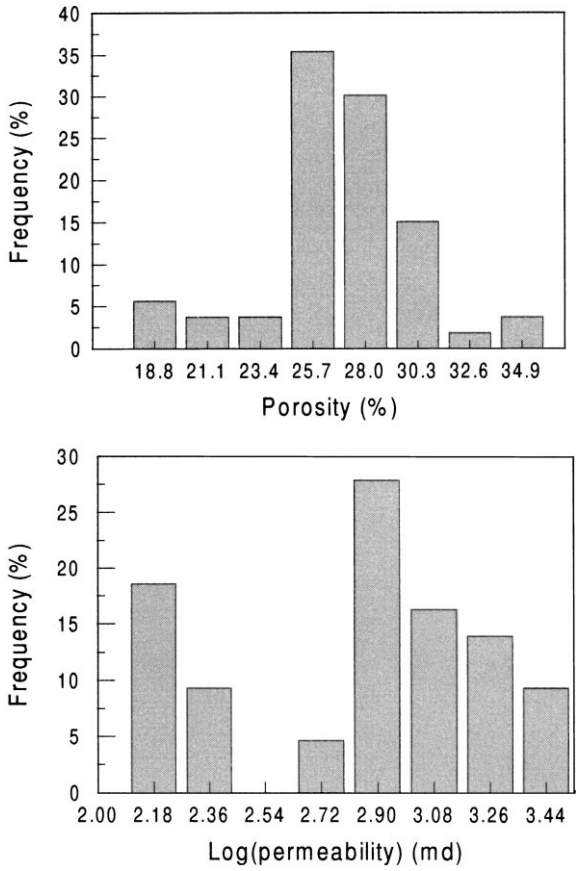


Fig. 8. Porosity, clay content and intrinsic permeability estimated from well log measurements on a water well drilled in Bahia, Brazil.

conditions and the mud filtrate invaded zone in the reservoir rock; (ii) the self-potential log and the natural gamma ray curve; and (iii) the sonic log converted to a total porosity curve. The resisitivity of the groundwater was measured directly on samples ($\rho_w = 70\ \Omega$ m), whereas that of the mud filtrate was estimated from the mud resistivity and from the SP deflection ($\rho_{mf} = 30.3\ \Omega$ m).

Both $\sigma_{cs}$ and $F$ were determined using Eq. (7) written for the flushed and the virgin conditions, respectively. The clay volume fraction $p$ was computed from Eq. (9) with $\sigma_{sh} = 0.085$ S/m a value close to that of a kaolinitic aggregate. The computed $p$ is in good agreement with $V_{cl}$ estimated from the gamma ray log using a conventional empirical equation (Asquith, 1990). Effective porosities were derived from the formation resistivity factor using an average $m$ equal to 1.83 (Börner et al., 1993). The sonic porosities are too high as compared to $\phi_e$, suggesting the sandstones are weakly compacted and the sonic data requires corrections before the application of Wyllie formula (Jorden and Campbell, 1986). Permeability values were computed with Eq. (30) using $\alpha_0$ and $q$ as determined for the sandstone samples (Vinegar and Waxman, 1984). In general, the computed $k$ are in a range from 100 to 2200 md with the more frequent values laying between 1000 and 2000 md. This range compares favorably with core measurements on true sandstone samples as described above.

In Fig. 9 we show a time-domain Schlumberger IP-resistivity sounding made over the São Sebastião Formation using a SYSCAL R2 resistivity-meter. The apparent resistivity data were inverted using a non-linear least square procedure based on horizontally layered earth model (Koefoed, 1979). As shown

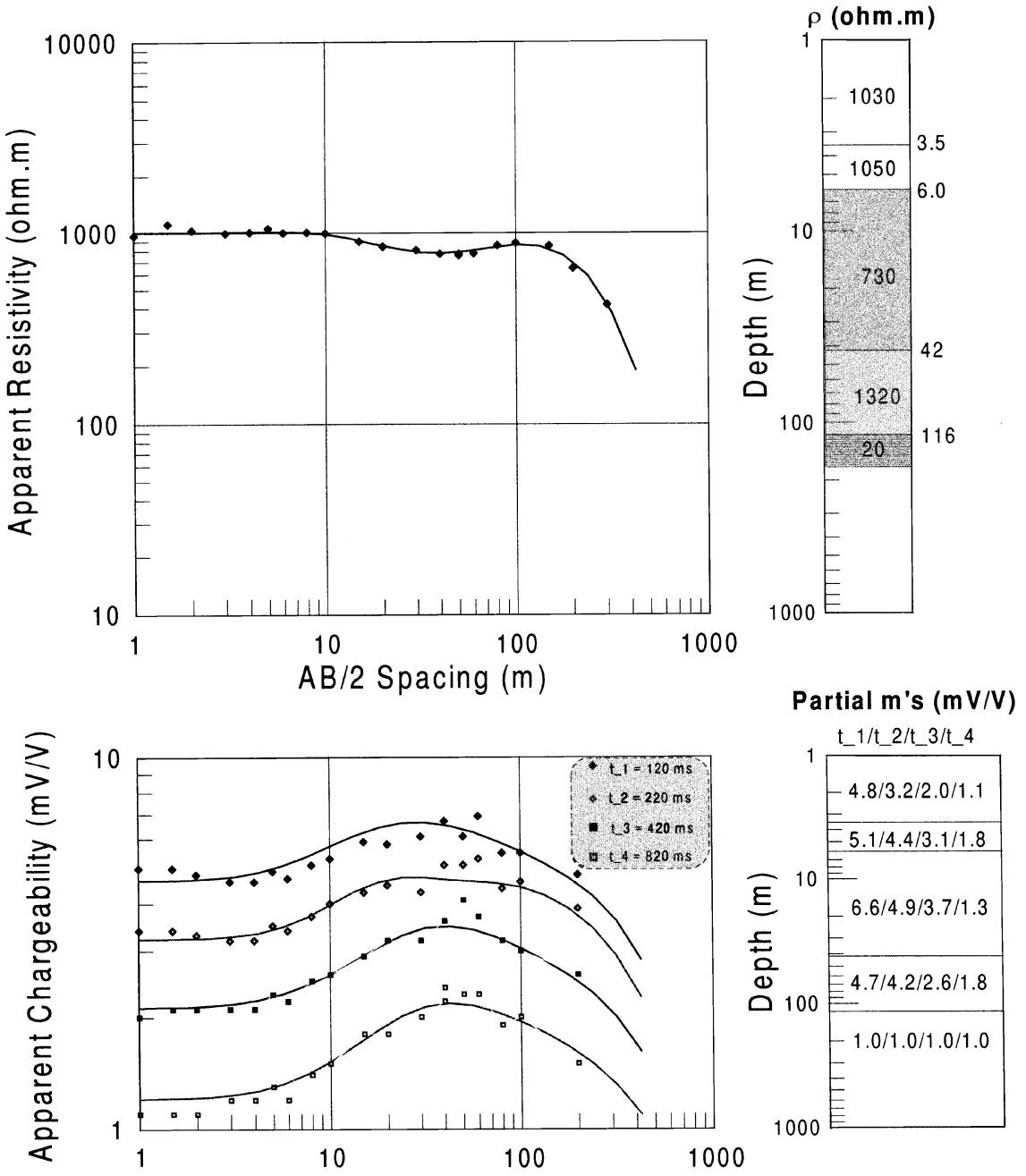


Fig. 9. Geoelectrical sounding data used in the petrophysical interpretation of shaly sandstone aquifer in Bahia, Brazil.

on the upper part of the figure the experimental data has been satisfactorily fitted to a five layers earth model. The two upper layers are in the top soil above the water table. The main aquifer includes the two next layers with resistivities of 730 and 1320 Ω m. Below 116 m the aquifer is underlain by a sequence dominated by shales (20 Ω m).

Simultaneously, partial apparent chargeabilities

were measured at four IP windows centered at 120, 220, 420 and 820 ms, as depicted in the bottom of Fig. 9. These data sets were interpreted using the quasi-linear geoelectrical approximation developed by Patella (1973). In his work Patella introduced a ficticious apparent resistivity ($\rho'_a$) for the Schlumberger array expressed as

$$\rho'_a = M_a \rho_a, \tag{31}$$

where $\rho_a$ is the usual apparent resistivity function. The analytic expression he found for $\rho'_a$ is formally equivalent to that of the conventional $\rho_a$. Thus, because $\rho'_i = M_i \rho_i$, we can use the same iterative procedure for inversion of $\rho_a$ to invert the apparent chargeability data.

The model geometry was fixed according to the apparent resistivity interpretation, and the inversion scheme was applied to find the partial $M_i$'s for the different layers. The best-fit chargeability models are shown on the right bottom of Fig. 9. Then, these partial values were used to obtain a close estimate for the *intrinsic* chargeability of the layers.

For each layer the partial chargeabilities were approximately described by an exponential function $M(t) = M_0 \exp(-t/\tau)$, where $M_0$ can be taken as the peak chargeability and $\tau$ as an average relaxation time for the induced polarization in the layer. By this way we find for the two aquifer layers $M_0(3) = 8.7$ mV/V and $M_0(4) = 5.4$ mV/V. These results were converted to FE's and then to phase shifts using Eqs. (20) and (19), the latter written assuming a 100 times frequency variation. The true bulk resistivities and the $\theta$ values of the layers allows to find their $\sigma_{0,I}$'s. From Eq. (16) we found the $\sigma_{cs,R}$'s using $\lambda_q = 0.0061$, a value extrapolated from the data of Figs. 3 and 4, for a NaCl electrolyte of 0.001 M salinity ($\rho_w = 70\ \Omega$ m). Finally using Eq. (30) together with the following petrophysical parameters for the sandstones $\phi_e = 25\%$, $m = 1.83$, $\delta_c = 100\ m/S$, and $\alpha_0 = 180,\ 015$ md and $q = 2.78$, as found for the Vinegar and Waxman data, we obtain $k_3 = 1500\ md$ and $k_4 = 1750\ md$ for the permeabilities of these two sandstone bodies.

## 3. Conclusions

We briefly review and expand the theory proposed by de Lima and Sharma (1990, 1992) to describe the electrical properties of shaly sandstones. We have shown both theoretically and with experimental data that the electrical resistivity and the induced polarization parameters carry direct information about the volume conductivity of the sandstone matrix. Thus, the well log measurements obtained with tools having different depths of investigation, as well as surface IP-resistivity measurements can be used to find $F$, $\sigma_{cs}$ and $p$ for shaly sandstone formations. Practical application of these procedures shows good agreement with estimates based on different approaches and with experimental measurements on samples.

We have also developed a new procedure for predicting the permeability of sandstones based on petrophysical parameter readily extractable from electrical logs and surface geoelectrical measurements. We derive a Kozeny–Carman type equation from first principles, showing the remarkable influence of a lithoporosity factor—the combination of a geometrical porosity–tortuosity term, with a length pore scale, clay type and volume content in the sandstone matrix, as expressed by the factor $\delta_c \sigma_{cs}$. In this treatment the hydraulic tortuosity is determined as the average electrical tortuosity along the free pore electrolyte. The equation was firmly tested with experimental data measured on different shaly sandstone samples published by Vinegar and Waxman (1984). Next, it was applied as a first approximation to estimate sandstone permeabilities from electrical logs and surface geoelectrical sounding measurements. The inferred values compare consistently with the sample measurements. These estimated values of permability can easily be converted to that of hydraulic conductivity to be used for groundwater management.

## Acknowledgements

We wish to thank the Brazilian agencies Financiadora de Estudos e Projetos (FINEP) and the National Council for Scientific Development (CNPq) for providing the financial support for this work. We would like to thank H. Sato and B. Clennell for the critical revision of this manuscript.

## References


Archie, G.E., 1950. Introduction to petrophysics of resevoir rocks. Bull. AAPG 34, 943–961.

Asquith, G., 1990. Log evaluation of shaly sandstones: a practical guide. Am. Assoc. Petr. Geol., Course Notes No. 31.

Bodmer, R., Ward, S.H., Morrison, H.F., 1968. On induced electrical polarization and groundwater. Geophysics 33, 805–821.

Börner, F., Gruhne, M., Schön, J., 1993. Contamination indications derived from electrical properties in the low frequency range. Geophys. Prosp. 41, 83–89.

Börner, F.D., Schopper, J.R., Weller, A., 1996. Evaluation of transport and storage properties in the soil and groundwater zone from induced polarization measurements. Geophys. Prosp. 44, 583–601.

Brace, W.F., 1977. Permeability from resistivity and pore shape. J. Geophys. Res. 82, 3343–3349.

Carman, P.C., 1956. Flow of Gases Through Porous Media, Butterworth, London.

Clennell, B., 1997. Tortuosity: a guide through the maze Special Publication 1997. In: Lovell, M.A., Harvey, P.K. (Eds.). Developments in Petrophysics, Geological Society, London, p. 122.

Cremers, A.E., Laudelout, H., 1966. Surface mobilities of cations in clays. Proc. Soil Sci. Soc. Am. 30, 570–576.

Croft, M.G., 1971. method of calculating permeability from electric logs. US Geol. Surv., Prof. Paper 750, 265–269.

Clavier, C., Coates, G., Dumanoir, J., 1997. The theoretical and experimental bases for the "dual water" model for the interpretation of shaly sands. 52nd Ann. Fall Tech. Conf., Soc. Petr. Engr., Paper SPE. 2961.

de Lima, O.A.L., Sharma, M.M., 1990. A grain conductivity approach to shaly sands. Geophysics 50, 1347–1356.

de Lima, O.A.L., Sharma, M.M., 1992. A generalized Maxwell–Wagner theory for membrane polarization in shaly sands. Geophysics 57, 431–440.

de Lima, O.A.L., 1993. Geophysical evaluation of sandstone aquifers in the Recôncavo-Tucano Basin, Bahia—Brazil. Geophysics 58, 1689–1702.

de Lima, O.A.L., 1995. Water saturation and permeability from resistivity, dielectric and porosity logs. Geophysics 60, 1756–1764.

Dias, C.A., 1972. Analytical model for a polarizable medium at radio and lower frequencies. J. Geophys. Res. 77, 4945–4956.

Fricke, H., 1924. mathematical treatment of the electrical conductivity and capacity of disperse system. Phys. Rev. 24, 575–587.

Haring, R.E., Greenkorn, R.A., 1970. statistical model of a porous medium with nonuniform pores. Am. Inst. Chem. Eng. J. 16, 477–483.

Heigold, P.C., Gilkeson, R.H., Castwright, K., Reed, P.C., 1980. Aquifer transmissivity from surficial electrical measurements. Groundwater 17, 330–345.

Hubbert, M.K., 1940. The theory of groundwater motions. J. Geology 48, 785–944.

Jorden, J.R., Campbell, F.L., 1986. Well Logging II—Electric and Acoustic Logging. Soc. Petr. Eng., Mono. 10 H. L. Doherty Series.

Katz, A.J., Thompson, A.H., 1985. Fractal sandstone pores: implications for conductivity and pore formation. Phys. Rev. Lett. 54, 1325–1328.

Kelly, W.E., 1977. Geoelectric sounding for estimating hydraulic conductivity. Ground Water 15, 420–425.

Klein, J.D., Sill, W.R., 1982. Electrical properties of artificial clay-bearing sandstone. Geophysics 47, 1593–1605.

Koefoed, O., 1979. Geosounding Principles 1—Resistivity Sounding Measurements, Elsevier, Amsterdam.

Korvin, G, 1992. Fractal Models in Earth Sciences, Elsevier, Amsterdam.

Kosinski, W.K., Kelly, W.E., 1981. Geoelectric soundings for predicting aquifer properties. Ground Water 19, 163–171.

Marshall, D.J., Madden, T.R., 1959. Induced polarization, a study of its causes. Geophysics 24, 790–816.

Mualem, Y., Friedman, S.P., 1991. Theoretical prediction of electrical conductivity in saturated and unsaturated soil. Water Resour. Res. 27, 2771–2777.

Ogilvy, A.A., Kuzmina, E.N., 1972. Hydrogeologic and engineering-geologic possibilities for employing the method of induced potencials. Geophysics 37, 839–861.

Patella, D., 1973. new parameter for the interpretation of induced polarization field prospecting (time-domain). Geophys. Prosp. 21, 315–329.

Scheidegger, A.E., 1974. The physics of flow through porous Media. 3rd ed. University of Toronto Press.

Shuey, R.T., Johnson, M., 1973. On the phenomenology of electrical relaxation in rocks. Goephysics 38, 37–48.

Scott, T.D., C. Purdy, C., 1988. Log derived permeability and flushed zone saturation utilising high frequency electromagnetic wave attenuation and propagation time. 29th Ann. Log. Symp. Trans., Soc. Prof. Well Log Analysts, Paper I.

Sen, P.N., Straley, C., Kenion, W.E., Whittingham, M.S., 1990. Surface-to-volume ratio, charge density, nuclear magnetic relaxation, and permeability in clay-bearing sandstones. Geophysics 55, 61–69.

Sighal, D.C., Sri Niwas, Shaked, M., Adam, E.M., 1998. Estimation of hydraulic characteristics of alluvial aquifers from electrical resistivity data. J. Geol. Soc. India 51, 165–183.

Sri Niwas, Singhal, D.C., 1981. Estimation of aquifer transmissivity from Dar-Zarrouk parameters in porous media. Hydrol. J. 50, 393–399.

Sri Niwas, Singhal, D.C., 1985. Aquifer transmissivity of porous media from resistivity data. Hydrol. J. 82, 143–153.

Terzaghi, K.V., 1955. Influence of geological factors on the engineering properties of sediments. Econ. Geol. 15, 557–618.

Turcotte, D.L., 1992. Fractals and Chaos in Geology and Geophysics, Cambridge University Press, New York.

Vacquier, V., Holmes, C.R., Kintzinger, P.R., Lavergne, M., 1957. Prospecting for ground water by induced electrical polarization. Geophysics 22, 660–687.

Vinegar, H.J., Waxman, M.H., 1984. Induced polarization of shaly sands. Geophysics 49, 1267–1287.

Yadav, G.S., Abolfazli, H., 1998. Geoelectrical soundings and their

relationship to hydraulic parameters in semiarid regions of Jalore, Northwestern India. J. Appl. Geophys. 39, 35–51.

Zonge, K.L., Sauck, W.A., Sumner, J.S., 1972. Comparison of time, frequency, and phase measurements in induced polarization. Geophys. Prosp. 20, 626–648.

Weerts, A.H., Bouten, W., Verstraten, J.M., 1999. Simultaneous measurement of water retention in soil: testing the Mualem–Friedman tortuosity model. Water Resour. Res. 35, 1781–1787.

Weller, A., Börner, F.D., 1996. Measurements of spectral induced polarization for environmental purposes. Environ. Geol. 27, 329–334.

Winsauer, W.O., Shearin, H.M., Masson, P.H., Williams, M., 1952. Resistivity of brine-saturated sands in relation to pore geometry. Bull. Am. Ass. Pet. Geol. 36, 253–277.

Wong, P., Koplik, J., Tomanic, J.P., 1984. Conductivity and permeability of rocks. Phys. Rev. B 30, 6604–6614.

Worthington, P.F., Collar, F.A., 1984. The relevance of induced polarization to quantitative formation evaluation. Marine and Petr. Geol. 1, 14–26.

Wyllie, M.R.J., Rose, W.D., 1950. Some theoretical considerations related to quantitative evaluation of the physical characteristics of reservoir rock from electric log data. Trans. Am. Inst. Mech. Engng 189, 105–118.

Wyllie, M.R.J., Spangler, M.B., 1952. Application of electrical resistivity measurements to problems of fluid flow in porous media. Bull. Am. Assoc. Petr. Geol. 36, 359–403.